Chemistry & Biology
Article

Methionine Aminopeptidases from *Mycobacterium tuberculosis* as Novel Antimycobacterial Targets

Omonike Olaleye,[1,2,6] Tirumalai R. Raghunand,[4,7] Shridhar Bhat,[1] Jian He,[1] Sandeep Tyagi,[4] Gyanu Lamichhane,[4] Peihua Gu,[5] Jiangbing Zhou,[5] Ying Zhang,[5] Jacques Grosset,[4] William R. Bishai,[4] and Jun O. Liu[1,3,*]
[1]Department of Pharmacology and Molecular Sciences, Johns Hopkins School of Medicine, Baltimore, MD 21205, USA
[2]Department of Pharmaceutical Sciences, College of Pharmacy and Health Sciences, Texas Southern University, Houston, TX 77004, USA
[3]Department of Oncology, Johns Hopkins School of Medicine, Baltimore, MD 21205, USA
[4]Center for Tuberculosis Research, Johns Hopkins School of Medicine, Baltimore, MD 21231, USA
[5]Department of Molecular Microbiology and Immunology, Bloomberg School of Public Health, Johns Hopkins University, Baltimore, MD 21205, USA
[6]Present address: College of Pharmacy and Health Sciences, Texas Southern University, Houston, TX 77004, USA
[7]Present address: Center for Cellular and Molecular Biology, Hyderabad, India
*Correspondence: joliu@jhu.edu
DOI 10.1016/j.chembiol.2009.12.014

SUMMARY

Methionine aminopeptidase (MetAP) is a metalloprotease that removes the N-terminal methionine during protein synthesis. To assess the importance of the two MetAPs in *Mycobacterium tuberculosis*, we overexpressed and purified each of the MetAPs to near homogeneity and showed that both were active as MetAP enzymes in vitro. We screened a library of 175,000 compounds against *Mt*MetAP1c and identified 2,3-dichloro-1,4-naphthoquinone class of compounds as inhibitors of both *Mt*MetAPs. It was found that the *Mt*MetAP inhibitors were active against replicating and aged nongrowing *M. tuberculosis*. Overexpression of either *Mt*MetAP1a or *Mt*MetAP1c in *M. tuberculosis* conferred resistance of bacterial cells to the inhibitors. Moreover, knockdown of *Mt*MetAP1a, but not *Mt*MetAP1c, resulted in decreased viability of *M. tuberculosis*. These results suggest that *Mt*MetAP1a is a promising target for developing antituberculosis agents.

INTRODUCTION

Mycobacterium tuberculosis (*M. tuberculosis*), the etiological agent of tuberculosis, is among the oldest pathogens that have affected humans globally, and the re-emergence of *M. tuberculosis* has become a primary public health burden (Dye, 2006; Gandhi et al., 2006; Raviglione, 2003; Zignol et al., 2006). The rise in multidrug-resistant and extensively drug-resistant strains of *M. tuberculosis* has reduced the effect of current treatment options (Cole et al., 1998; Fauci, 2008; Zhang, 2005). Thus, the development of antibiotics with novel mechanisms of action is essential to effectively treating patients with tuberculosis (TB).

Methionine aminopeptidase (MetAP) is a dinuclear metalloprotease that removes the N-terminal methionine from nascent proteins (Giglione et al., 2003; Lowther and Matthews, 2000). MetAP is conserved in all life forms from bacteria to humans. There are two classes of MetAPs, MetAP1 and MetAP2, which differ in the presence of an internal polypeptide insertion present within the catalytic domain of MetAP2 (Arfin et al., 1995). Eukaryotes possess both classes, whereas prokaryotes have homologs of either MetAP1 (eubacteria) or MetAP2 (archaeabacteria) (Lowther and Matthews, 2000). Variants of MetAP1 are further classified as MetAP1a, MetAP1b, and MetAP1c (Addlagatta et al., 2005b), which are distinguished by the existence of an N-terminal extension in MetAP1b and MetAP1c, and a unique zinc finger domain in MetAP1b. Recently, we solved the X-ray crystal structures of the apo- and methionine-bound forms of *M. tuberculosis* MetAP1c (Addlagatta et al., 2005b). The structure revealed the existence of a highly conserved proline rich N-terminal extension in *Mt*MetAP1c that is absent in *Mt*MetAP1a but has sequence homology with the linker region of human MetAP1 (*Hs*MetAP1) (Addlagatta et al., 2005a).

Genetic studies have shown that deletion of *MetAP* from *Escherichia coli* and *Salmonella typhimurium* is lethal (Chang et al., 1989; Miller et al., 1989). In yeast, deletion of either *metAP1* or *metAP2* results in a slow-growth phenotype, whereas disruption of both genes is lethal (Chang et al., 1992; Li and Chang, 1995). In *Caenorhabditis elegans*, MetAP2 is essential for germ cell development (Boxem et al., 2004). In mammalian cells, both *Hs*MetAP1 and *Hs*MetAP2 have been shown to be required for cell proliferation (Bernier et al., 2005). In particular, *Hs*MetAP2 is essential for endothelial cell growth and angiogenesis and mediates the inhibition of endothelial cells by the fumagillin family of natural products (Griffith et al., 1997; Sin et al., 1997; Yeh et al., 2006). Recent studies have also shown that *Hs*MetAP1 is involved in regulating cell cycle progression in mammalian cells (Hu et al., 2006).

The essential role of MetAPs in prokaryotes makes this enzyme an attractive target for the development of new antibiotics. In prokaryotes, where protein synthesis begins with an N-formylated methionine, peptide deformylase (PDF) catalyzes the removal of the formyl group before MetAP removes the newly unmasked N-terminal methionine (Giglione et al., 2003; Solbiati et al., 1999). Unlike most other prokaryotes, *M. tuberculosis* possesses two MetAPs, *Mt*MetAP1a and *Mt*MetAP1c, which


```
MtMetAP1c       ------------------MPSRTALSPGVLS---------------------------- 13
HsMetAP1        MAAVETRVCETDGCSSEAKLQCPTCIKLGIQGSYFCSQECFKGSWATHKLLHKKAKDEKA 60
MtMetAP1a       ------------------------------------------------------------
EcMetAP1        ------------------------------------------------------------

MtMetAP1c       ----------------------------------PTRPVPNWIARPEYVGKPAAQEGSEP 39
HsMetAP1        KREVSSWTVEGDINTDPWAGYRYTGKLRPHYPLMPTRPVPSYIQRPDYADHPLGMSESEQ 120
MtMetAP1a       ----------------------------------MRPLARLRGRRVVPQR--------- 16
EcMetAP1        ---------------------------------------------MIICK--------- 5

MtMetAP1c       WVQ--------TPEVIEKMRVAGRIAAGALAEAGKAVAPGVTTDELDRIAHEYLVDNGAY 91
HsMetAP1        ALKGTSQIKLLSSEDIEGMRLVCRLAREVLDVAAGMIKPGVTTEEIDHAVHLACIARNCY 180
MtMetAP1a       ----------SAGELDAMAAAGAVVAAALRAIRAAAAPGTSSLSLDEIAESVIRESGAT 65
EcMetAP1        ----------TPRELGIMREAGRIVALTHEELKKHIKPGISTKELDQIAERFIKKQGAI 54

MtMetAP1c       PSTLGYKGFPKSCCTSLNEVICHGIPD-STVITDGDIVNIDVTAYIGGVHGDTNATFPAG 150
HsMetAP1        PSPLNYYNFPKSCCTSVNEVICHGIPD-RRPLQEGDIVNVDITLYRNGYHGDLNETFFVG 239
MtMetAP1a       PSFLGYHGYPASICASINDRVVHGIPSTAEVLAPGDLVSIDCGAVLDGWHGDAAITFGVG 125
EcMetAP1        PSFKGYNGFRGSICVSVNEELVHGIPG-SRVLKDGDIISIDIGAKLNGYHGDSAWTYPVG 113
                                                  *         *

MtMetAP1c       DVADEHRLLVDRTREATMRAINTVKPGRALSVIGRVIESYANRFG------YNVVRDFTG 204
HsMetAP1        EVDDGARKLVQTTYECLMQAIDAVKPGVRYRELGNIIQKHAQANG------FSVVRSYCG 293
MtMetAP1a       ALSDADEALSEATRESLQAGIAAMVVGNRLTDVAHAIETGTRAAELRYGRSFGIVAGYGG 185
EcMetAP1        NISDDDKKLLEVTEESLYKGLQEAKPGERLSNISHAIQTYVENEQ------FSVVREYVG 167

MtMetAP1c       HGIGTTFHNGLVVLHYDQPAVETIMQPGMTFTIEPMINLGALDYEIWDDGWTVVTKDRKW 264
HsMetAP1        HGIHKLFHTAPNVPHYAKNKAVGVMKSGHVFTIEPMICEGGWQDETWPDGWTAVTRDGKR 353
MtMetAP1a       HGIGRQMHMDPFLPNEGAPGRGPLLAAGSVLAIEPMLTLGTTKTVVLDDKWTVTTADGSR 245
EcMetAP1        HGVGQDLHEDPQIPHYGPPNKGPRLKPGMVLAIEPMVNAGSRYVKTLADNWTVVTVDGKK 227
                *                                 *

MtMetAP1c       TAQFEHTLLVTDTGVEILTCL------------ 285
HsMetAP1        SAQFEHTLLVTDTGCEILTRRLDSARPHFMSQF 386
MtMetAP1a       AAHWEHTVAVTDDGPRILTLG------------ 266
EcMetAP1        CAHFEHTIAITETGFDILTRV------------ 248
                    *
```

Figure 1. Sequence Comparison of *Mt*MetAP1a, *Mt*MetAP1c, *Hs*MetAP1 and *Ec*MetAP1

The alignment was generated using ClustalW (www.ebi.ac.uk). Both *Mt*MetAPs share a 33% similarity, and the metal-chelating residues necessary for catalysis are conserved (*). *Mt*MetAP1a and *Ec*MetAP1 lack the N-terminal extension with a PXXPXP motif present in *Mt*MetAP1c AND *Hs*MetAP1 (underlined).

share about 33% sequence identity (Figure 1). Both *Mt*MetAPs have less than 45% similarity to *E. coli* MetAP1 (*Ec*MetAP1), less than 48% similarity to human MetAP1 (hMetAP1), and less than 30% similarity to human MetAP2 (hMetAP2). Given the presence of the two MetAP genes in *M. tuberculosis*, it was unclear whether inhibition of either or both *Mt*MetAPs is sufficient to inhibit TB growth.

Recently, we and others (Zhang et al., 2009) characterized both MetAPs from *M. tuberculosis* strains CDC1551 and H37Rv, respectively. In this study, we investigated the functional importance of the two *Mt*MetAPs using a combination of chemical and genetic approaches. We began by overexpressing and purifying the two *Mt*MetAPs to near homogeneity from *E. coli.* Biochemical characterization revealed that both *Mt*MetAPs are functional as methionine aminopeptidases in vitro. Using a high-throughput screening approach, we screened 175,000 compounds against *Mt*MetAP1c and identified compounds with 2,3-dichloro-1,4-naphthoquinone core structure as inhibitors. We found that these inhibitors were active against both *Mt*MetAP enzymes and mycobacterial growth in culture. In addition, we obtained genetic evidence that an *Mt*MetAPs is likely the relevant target of the newly discovered inhibitors in *M. tuberculosis* in culture.

RESULTS

Overexpression, Purification, and Characterization of *Mt*MetAP1a and *Mt*MetAP1c

A BLAST search of the genome of *M. tuberculosis* (Cole et al., 1998) revealed the existence of two orthologs of *E. coli* MetAP, and their N-terminal extension suggested that they belonged to *Mt*MetAP1a and *Mt*MetAP1c classes, respectively (Figure 1) (Addlagatta et al., 2005b). Previously, we have succeeded in

cloning, overexpressing, and purifying recombinant *Mt*MetAP1c with an N-terminal poly-histidine tag for crystallographic studies (Addlagatta et al., 2005b). Recombinant *Mt*MetAP1a was overexpressed and purified in a similar manner, except that the expression vector pET-28b was used to append a C-terminal poly-His tag on the protein. Both proteins were efficiently purified to near homogeneity by immobilized metal affinity chromatography using Talon resins. Upon purification, C-terminally poly-His-tagged *Mt*MetAP1a and N-terminally poly-His-tagged *Mt*MetAP1c were seen at about 28 kDa and 32 kDa, respectively, on Coomassie blue-stained SDS-polyacrylamide gels (Figures 2A and 2B). The average yield from 1 liter of *E. coli* culture for *Mt*MetAP1a and *Mt*MetAP1c were 4.3 and 13 mg, respectively.

The enzymatic activities of the purified *M. tuberculosis* MetAPs were assessed using a chromogenic substrate (Met-Pro-pNA) in a coupled enzymatic assay with proline aminopeptidase as the coupling enzyme (Zhou et al., 2000). Both purified recombinant proteins were found to be catalytically active in this assay (Figure 2C). The kinetic constants for *Mt*MetAP1a and *Mt*MetAP1c were determined by measuring enzyme activity at different substrate concentrations ranging from 0 to 800 μM. The K_m for the artificial substrate was similar for both enzymes, whereas the k_{cat} for *Mt*MetAP1c was 10-fold higher than that for *Mt*MetAP1a (Table 1).

Using the same enzymatic assay, we also determined the effects of temperature on both enzymes (see Figure S1 available online). The temperature profile of *Mt*MetAP1a gave a bell-shaped curve, with an optimal temperature of 42°C. In contrast, the activity of *Mt*MetAP1c increased by smaller increments as temperatures were increased from 4°C to 50°C before loss of activity was seen at 65°C. These results suggested that *Mt*MetAP1c had a slightly higher thermostability than did *Mt*MetAP1a. The pH profiles of both *Mt*MetAPs were determined by measuring the enzymatic activity in different buffers. The optimal pH for both *Mt*MetAPs was found to be 8.0 using 50 mM HEPES as buffer (Figure S2). It is noteworthy that *Mt*MetAP1a had optimal activity from pH 6.5 to pH 8.0, whereas *Mt*MetAP1c had a much steeper decline in activity upon pH changes from 8.0.

Because the physiological metal cofactor for MetAPs remains controversial, we determined the metal dependence of the two *Mt*MetAPs. Both *Mt*MetAPs were found to be active in the presence of Co^{2+} or Mn^{2+}. For *Mt*MetAP1c, concentration-dependent inhibition was observed in the presence of increasing amounts of $CoCl_2$ (Figure S3A). In contrast, *Mt*MetAP1c retained its optimal activity in the presence of 0.1–10 μM of Mn^{2+}, and only a slight decrease in activity was seen when Mn^{2+} concentration was increased beyond 100 μM (Figure S3B). Unlike *Mt*MetAP1c, *Mt*MetAP1a showed optimal activity at 10 μM of Co^{2+} (Figure S3C) and 0.1–1 mM of Mn^{2+} (Figure S3D).

Identification of *Mt*MetAP Inhibitors via High-Throughput Screening

In collaboration with ASDI Inc., we screened a structurally diverse small molecule library of 175,000 compounds against *Mt*MetAP1c at a final concentration of 30 μM in 384-well plates using the coupled enzymatic assay (Zhou et al., 2000). A total of 439 hits were identified that exhibited greater than 40% inhibition of *Mt*MetAP1c at a final concentration of 10 μM. Interestingly, a number of the hits were found to contain 2,3-dichloro-1,4-napthoquinone core structure. We acquired a total of 28 structural analogs for structure-activity relationship studies (Table 2). For *Mt*MetAP1a, we found that substitutions to the 2, 3-dichloro positions reduced activity, except for the 2,3-dibromo derivative (compound **20**; Table 2). In contrast, *Mt*MetAP1c tolerated both fluorophenoxy and dibromo substitutions to the 2,3-dichloro positions (compounds **21**, **22**, and **20**, respectively) (Table 2). In addition, we also determined the effects of some naturally occurring 1,4-naphthoquinones and vitamin K derivatives (Table 2) against both *Mt*MetAP1a and *Mt*MetAP1c. None of them was active against either *Mt*MetAP enzyme. Among all analogs we obtained and tested, 2,3-dibromo-1,4-naphthoquinone (compound **20**) was found to be most potent against both *Mt*MetAP1a and *Mt*MetAP1c with IC_{50} values of around 1 μM (Table 2).

Next, we determined the effects of the most potent inhibitors on the growth *M. tuberculosis* in culture. Compounds **4** and **20** were found to be most potent against *M. tuberculosis* with minimum inhibitory concentration (MIC) values of 10.0 and 10.0–25 μg/mL, respectively (Table 3). Interestingly, the other analogs with slightly higher IC_{50} values for either *Mt*MetAP1c (compounds **2** and **3**) or *Mt*MetAP1a (compounds **21** and **22**) showed about a two-fold increase in MIC values (Table 3). In addition to replicating *M. tuberculosis*, we also tested these *Mt*MetAP inhibitors in aged nongrowing *M. tuberculosis* (Table 3). Interestingly, the active inhibitors, compounds **4** and **20**, were equally effective against the aged non-growing form of *M. tuberculosis* as the replicating form.

Overexpression of *Mt*MetAP1a or *Mt*MetAP1c Confers Resistance to *M. tuberculosis* to the Newly Identified MetAP Inhibitors

If either of the *Mt*MetAPs is the target of the inhibitors in vivo, it is expected that their overexpression will cause resistance. To perturb the cellular levels of *Mt*MetAPs, we first cloned each of the mycobacterial MetAP1s into pSCW35ΔsigF (Figure 3), a vector whose promoter is regulated by acetamide (P_{ace}). This vector also has an *attP* site that allows for stable integration of a single copy of the plasmid into the *attB* site in the chromosome of *M. tuberculosis* (Raghunand et al., 2006). The entire ORFs of *Mt*MetAP1a and *Mt*MetAP1c genes were amplified by PCR from *M. tuberculosis* strain CDC1551 genomic DNA and were then subcloned into pSCW35ΔsigF vector in the sense orientation. The pSCW35-(*Mt*MetAP1a) and pSCW35-(*Mt*MetAP1c) clones were verified by DNA sequencing.

To overexpress *Mt*MetAP1a and *Mt*MetAP1c in *M. tuberculosis*, we constructed knock-in strains for both *Mt*MetAPs by transforming *M. tuberculosis* CDC1551 with pSCW35ΔsigF-(*Mt*MetAP1a) and pSCW35ΔsigF-(*Mt*MetAP1c), respectively. In addition, we also transformed *M. tuberculosis* with a control empty plasmid, pSCW35ΔsigF. All three transformants were grown until early logarithmic phase, and expression was induced by addition of 0.2% acetamide followed by incubation for an additional 24 hr. To confirm that the levels of both *Mt*MetAP1s were increased, we used real-time quantitative PCR to quantitate the transcript levels of both enzymes. The mRNA levels of *Mt*MetAP1a and *Mt*MetAP1c were about 4.5- and 6-fold higher than that of the control, respectively (Figure 3B). We examined

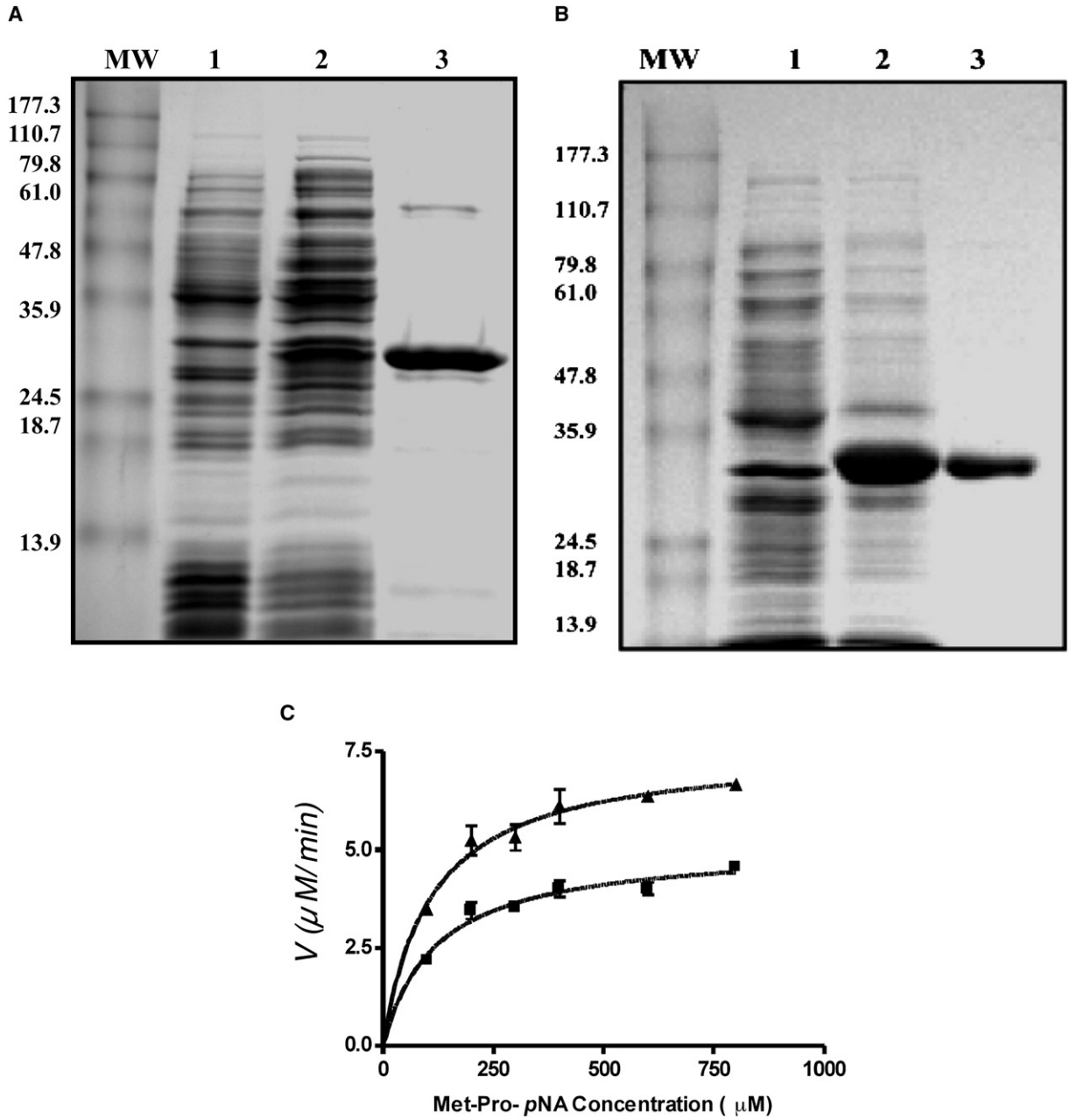

Figure 2. Purification and Kinetic Characterization of Recombinant MetAPs from *M. tuberculosis*

The recombinant *Mt*MetAP1s were overexpressed in *E. coli* BL21 cells and purified by affinity chromatography as described in Experimental Procedures.

(A) PolyHis-tagged-MtMetAP1c (~32 kDa).

(B) PolyHis-tagged-MtMetAP1a (~28 kDa). Lane 1, Molecular weight marker; lane 2, uninduced whole cell lysate; lane 3, induced cell lysate; and lane 4, purified polyHis-tagged *Mt*MetAP1. The gel was stained with Coomassie blue.

(C) Velocity versus substrate concentration plot for *Mt*MetAP1a (triangles) and *Mt*MetAP1c (squares). The kinetic constants were obtained by measuring enzyme activity at different substrate concentrations. The reactions were performed in 96-well plates at room temperature and monitored at 405 nm on a UV-Vis spectrophotometer. The total volume of reaction was 100 μl (each reaction contains 40 mM HEPES [pH 7.5], 100 mM NaCl, 1 μM CoCl2, 100 μg/mL BSA, 0.1 U/mL ProAP, and 0-800 μM Met-Pro-*p*NA), 334 nM *Mt*MetAP1c, and 3.29 μM *Mt*MetAP1a, respectively. The background hydrolysis was corrected. The data were from quadruplet experiments and were fitted against the Michealis-Menten equation: $V = Vmax \times [S] / (Km + [S])$, using the Graphpad prism software for one-site binding hyperbola.

the growth of the knock-in *M. tuberculosis* strains in the presence of 2,3-dichloro-1,4-naphthoquinone. Both the wild-type and control *M. tuberculosis* strains were inhibited in the presence of 10 μg/mL 2,3-dichloro-1,4-naphthoquinone (Figure 4). In contrast, both *Mt*MetAP1a and *Mt*MetAP1c knock-in strains gained resistance to the inhibitor (Figure 4), suggesting that

Table 1. Kinetic Constants for MetAPs from *M. tuberculosis*

Kinetic Constants	*Mt*MetAP1a	*Mt*MetAP1c
Km (μM)	122 ± 22	113 ± 31
k_{cat}/Km ($M^{-1}min^{-1}$)	1.3 × 10^4	2.0 × 10^5
V_{max} (μM/min)	5.1 ± 0.2	7.6 ± 0.5

The assay was performed in the presence of 1 μM $CoCl_2$. Details of the assay are described in Experimental Procedures.

both *Mt*MetAP1a and *Mt*MetAP1c are capable of binding and sequestering the inhibitor in vivo.

Knockdown of *Mt*MetAP1a, but Not *Mt*MetAP1c, Led to a Decrease in Growth of *M. tuberculosis*

It has been shown that MetAP plays an essential role in bacteria, because knockout in *E. coli* and other bacteria is lethal (Chang et al., 1989; Miller et al., 1989). Because *M. tuberculosis* possesses two MetAP genes, it was unclear whether knocking out either or both of these genes in *M. tuberculosis* is sufficient to inhibit growth. To study the requirement of *Mt*MetAP1a and *Mt*MetAP1c for viability of *M. tuberculosis*, we cloned each of the mycobacterial MetAP1s in the reverse orientation downstream of the acetamide-regulated promoter (P_{ace}) in pSCW35ΔsigF (Figure 3A). The resulting plasmids, pSCW35ΔsigF-(α-*Mt*MetAP1a) and pSCW35ΔsigF-(α-*Mt*MetAP1c), were verified by sequencing. These antisense vectors, as well as the empty control vector, were used to transform *M. tuberculosis.* The three transformants were grown until early log phase, at which point the antisense RNA was induced by addition of 0.2% acetamide followed by incubation for an additional 24 hr. The cultures were grown for three weeks on plates in the presence and absence of acetamide. To confirm that the levels of both mycobacterial MetAP1s were altered, we used real-time quantitative PCR to determine the transcript levels of both enzymes. The mRNA levels of *Mt*MetAP1a and *Mt*MetAP1c were reduced by about 1.7- and 2.3-fold in comparison to that of the control (Figure 3C). The colony counts after three weeks (Table 4) showed that knockdown of *Mt*MetAP1c in *M. tuberculosis* had a marginal effect on bacterial growth in comparison to the control, indicating that *Mt*MetAP1c is probably not essential for *M. tuberculosis* growth in vitro. In contrast, knockdown of *Mt*MetAP1a decreased the viability to 76.0% in comparison to culture expressing the control vector (Table 4). Because *Mt*MetAP1a was only partially knocked down and the degree to which its mRNA decreased is even less than that of *Mt*MetAP1c, this decrease in cell viability is significant, suggesting that *MtMetAP1a* is likely an essential gene in *M. tuberculosis* and that the inhibitory effects of the newly identified inhibitors on TB growth was likely to be mediated by inhibition of *Mt*MetAP1a.

DISCUSSION

In this study, we applied a combination of chemical and genetic approaches to investigate the functions of two isoforms of *Mt*MetAP and gathered strong evidence that *Mt*MetAP1a is essential for the growth of *M. tuberculosis* and a promising target for discovering and developing anti-TB agents. In addition, we also identified naphthoquinones as an active pharmacophore for developing inhibitors of *Mt*MetAP1. Inhibition of *Mt*MetAP1a by either small molecule inhibitors or expression of an antisense RNA targeting *Mt*MetAP1a led to significant inhibition of the growth of *M. tuberculosis* in culture, supporting the notion that *Mt*MetAP1a plays an essential role in *M. tuberculosis*.

The availability of a number of analogs of this structural class made possible a preliminary structure-activity relationship study. Among a variety fo 2.3-disubstituted naphthoquinones tested, the analogs with the highest potency contain either a chlorine (**4**) or bromine (**20**) substituent. There is also a correlation between the potencies of the analogs to inhibit *Mt*MetAP enzymes in vitro and their ability to inhibit bacterial growth. Thus, the two most potent inhibitors of *Mt*MetAP (**4** and **20**) also exhibited the lowest MIC values for inhibition of TB culture growth (Tables 2 and 3). Together with the antisense RNA knockdown results, these observations provide additional evidence that inhibition of mycobacterial growth is due to inhibition of the *Mt*MetAP1a.

According to genomic sequences available to date, *M. tuberculosis* possesses two MetAP-encoding genes, in contrast to most other prokaryotes, which harbor only a single gene for MetAP enzyme. In a previous study, biochemical purification of MetAP enzyme from *M. smegmatis* yielded a single protein, calling into question whether both of the putative MetAP genes are expressed and, if so, whether they are bona fide MetAP enzymes (Narayanan et al., 2008). Using RT-PCR, we were able to detect mRNA for both *Mt*MetAP proteins, indicating that they are actively transcribed in *M. tuberculosis*. Using purified recombinant *Mt*MetAP proteins, we demonstrated that both *Mt*MetAP1a and *Mt*MetAP1c are active enzymatically, even though *Mt*MetAP1a is ~10-fold less active. We note that while this manuscript was under review, Zhang et al. (2009) reported the biochemical characterization of both MetAPs from *M. tuberculosis* with similar observations. Where the two studies overlapped, however, there are some important differences. For example, the two MetAP proteins were found by Zhang et al. to be similar in enzymatic activity. The optimal temperature, metal ion concentrations, and pH for the recombinant proteins also differ to some extent. It is noteworthy that different assays were used in the two studies. We used a contiguous spectrophotometric assay with Met-Pro-pNA as a substrate, but Zhang et al. used methionine-containing oligopeptides as substrates (Zhang et al., 2009). The distinct substrates and the accompanying assay conditions may account for most, if not all, of the qualitative differences in kinetic parameters and temperature and pH dependence observed in the two studies.

The unique presence of two isoforms of MetAP enzymes in TB, in contrast to the majority of other prokaryotes, called into question whether one or both isoforms are essential for the viability of the mycobacteria. To assess this question, we performed a high-throughput screen against *Mt*MetAP1c and identified a family of structurally related inhibitors sharing a common 1,4-napthoquinone core. Although evaluation of additional structural analogs led to the identification of more potent inhibitors of *Mt*MetAP1c, none of the inhibitors of this structural class is selective toward either *Mt*MetAP1c or *Mt*MetAP1a. The lack of isoform specificity is consistent with the observation that overexpression of either *Mt*MetAP isoform conferred resistance to the inhibitor. The nonselective *Mt*MetAP inhibitors were capable of inhibiting

the growth of *M. tuberculosis*, suggesting that either or both *Mt*MetAP enzymes are essential for bacterial growth, leaving unanswered the question of whether the growth inhibition was mediated through one or both isoforms of *Mt*MetAP. Using knockdown with specific antisense RNA, we found that knockdown of *Mt*MetAP1a, rather than *Mt*MetAP1c, slowed growth of *M. tuberculosis* in culture, which suggests that inhibition of *Mt*MetAP1a may be responsible for growth inhibition by the small molecule inhibitors. However, these results are also consistent with an alternative possibility that the two MetAP1 proteins are functionally redundant and inhibition of both enzymes mediated the growth inhibition by the nonselective small molecule inhibitors. It is worth pointing out that both *MtMetAP* genes have been previously predicted to be essential for *M. tuberculosis* survival in vivo and pathogenicity (Ribeiro-Guimaraes and Pessolani, 2007). Together with the previous observation that the two genes are optimally expressed at different growth phases of *M. tuberculosis* (Zhang et al., 2009), it is possible that only *Mt*MetAP1a is required for growth in culture medium in vitro. The presence of multiple isoforms of MetAP-encoding genes has also been seen in some other pathogenic microorganisms. For example, *Bacillus anthracis* possesses three putative MetAP genes, and malaria contains four different isoforms of MetAPs (Chen et al., 2006). In comparison to most prokaryotes, *M. tuberculosis* is also unique in that it has to evade and propagate within human microphages. It will be interesting to determine whether *Mt*MetAP1c may play a role in the survival of *M. tuberculosis* within mammalian cells.

Of the two *Mt*MtMetAP enzymes, *Mt*MetAP1c contains an N-terminal ''linker'' region, whereas MetAP1a is free of the N-terminal domain similar to other prokaryotic MetAP enzymes (Figure 1). Using nearly homogeneous recombinant proteins, we found that *Mt*MetAP1a is catalytically 10-fold less active than *Mt*MetAP1c. This difference in activity appeared to be due to the use of the artificial tripeptide substrate, because similar activities were found when oligopeptide substrates were used (Zhang et al., 2009). In addition, we also observed some difference in thermostability, optimal pH, and dependence on metal ions. In comparison with *Mt*MetAP1c, *Mt*MetAP1a has a lower optimal temperature, a broader range of optimal pH values spanning one unit of pH, and a higher threshold of activation by metal ions. Although *Mt*MetAP1c contains an N-terminal SH3 ligand-containing extension, MetAP1a contains an internal insertion of six amino acids, in comparison with MetAP1c and human MetAP1. These differences in primary structure and the accompanying tertiary structures may account for part of the differences in activity, substrate specificity, and other biochemical properties of the two *Mt*MetAPs. It also raised the possibility of identifying inhibitors that are specific for *Mt*MetAP1a over *Mt*MetAP1c or human MetAP1 as leads for anti-TB drugs.

SIGNIFICANCE

The emergence of multidrug-resistant and extensively drug-resistant *Mycobacterium tuberculosis* strains has imposed a pressing need for antimycobacterials with novel mechanisms of action. Methionine aminopeptidases are evolutionarily conserved enzymes, and they play essential roles for the viability of both prokaryotes and eukaryotes. The functional importance of MetAP in *M. tuberculosis*, however, remained unclear, as it possesses two genes, *MtMetAP1a* and *MtMetAP1c*. By overexpressing each isoform in *E. coli* and purifying them to near homogeneity, we demonstrated that both recombinant *Mt*MetAP proteins are enzymatically active. Furthermore, quantitative RT-PCR analysis revealed that both proteins are expressed, at least at the mRNA level, in stationary cell culture. Using high-throughput screening, we identified inhibitors of both enzymes, which also inhibited the growth of mycobacteria in culture. Using antisense RNA, we found that the two isoforms are not functionally redundant. Although the more active *Mt*MetAP1c is dispensable, *Mt*MetAP1a appears to be required for mycobacterial growth in culture. Thus, *Mt*MetAP1a can serve as a target and the naphthoquinone-containing inhibitors can serve as leads for the development of new anti-TB agents.

EXPERIMENTAL PROCEDURES

Materials

The vectors pET28a and pET28b and the *E. coli* BL21 expression host were purchased from Novagen. The expression vector pSCW35ΔsigF, a pMH94-based vector, was constructed by Dr. Sam Woolwine. The iScript cDNA synthesis kit and the SYBR Green Supermix were purchased from Bio-Rad Laboratories. The *M. tuberculosis* cultures medium, Middlebrook 7H9, was purchased from Becton Dickinson. The Talon resin was from Clontech. Isopropyl β-D-thiogalactopyranoside (IPTG) was purchased from Sigma Aldrich. The structurally diverse compound library was provided by ASDI.

Subcloning of the Two MetAPs from *M. tuberculosis*

The N-terminal polyHis-tag *Mt*MetAP1c gene was amplified by polymerase chain reaction (PCR) from *M. tuberculosis* (CDC1551) genomic DNA using Taq polymerase. The *M. tuberculosis* (CDC1551 strain) genomic DNA was generously provided by Dr. William Bishai. The primers used were 5′-GCG GGA TCC CCT AGT CGT ACC GCG CTC−3′ and 5′-GCG CTC GAG CTA CAG ACA GGT CAG GAT C-3′ for forward and reverse directions, respectively. The PCR fragments were cloned into pET28a, using the BamHI and XhoI restriction sites, respectively.

The C-terminal polyHis-tag MTMAP1A gene was amplified by PCR from pET28a (MtMAP1a) plasmid (this plasmid was also subcloned from *M. tuberculosis* genomic DNA generously provided by Dr. William Bishai). The primers used were 5′-GCG CCA TGG GCC CAC TGG CAC GGC TGC GGG GTC−3′ and 5′-GCG CTC GAG ACC GAG CGT CAG AAT TCG GGG CCC-3′ for forward and reverse directions, respectively. The PCR fragments were cloned into pET28b, using the NcoI and XhoI restriction sites, respectively. Both *Mt*MetAP1a and *Mt*MetAP1c clones were confirmed by sequencing.

Overexpression and Purification of Recombinant MetAP from *M. tuberculosis*

E. coli BL21 cells (DE3) containing the expression plasmid were cultured at 37°C in 1 liter of Listeria broth (LB) containing 30 mg kanamycin until OD_{600} reached about 1.0. The expression of *Mt*MetAP1a was induced by addition of isopropyl β-D-thiogalactopyranoside (IPTG) to a final concentration of 1 mM followed by continued shaking of the culture flask at 280 rpm, at 16°C for 48 hr. The cells were harvested and washed with 1× PBS (137 mM NaCl, 2.7 mM KCl, 4.3 mM $Na_2HPO_4.7H_2O$, and 1.4 mM KH_2PO_4 [pH 7.3]). The cells were sonicated in +TG buffer (50 mM HEPES [pH 8.0], 0.5 M KCl, 10% glycerol, 5 mM imidazole, and 0.1% Triton X-100) with EDTA-free protease inhibitor tablets. The resulting lysate was centrifuged at 8000× *g* for 10 min. The supernatant was loaded onto pre-equilibrated (+TG buffer) Talon resin (Clontech). After equilibration for 30 min, the beads were washed three times with −TG buffer (50 mM HEPES [pH 8.0], 0.5 M KCl, and 5 mM imidazole). The enzyme was eluted with 100 mM imidazole in −TG buffer. The protein was quantified using the Bradford assay. The average yield for *Mt*MetAP1a was 4.3 mg/l of culture.

Table 2. Effect of Naphthoquinones on *Mt*MetAPsFx1

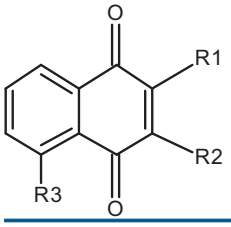

ID	R1	R2	R3	IC50 (μM) MtMetAP1a	MtMetAP1c
2	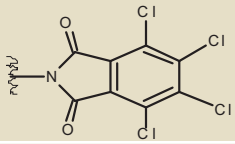	Cl	H	4.0 ± 0.3	8.7 ± 0.2
3	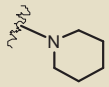	Cl	H	8.0 ± 1.31	7.2 ± 1.8
4	Cl	Cl	H	3.3 ± 0.3	6.6 ± 1.2
5	NH_2	Cl	H	>100	>100
6	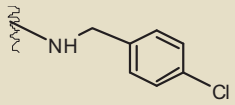	Cl	H	>100	>100
7	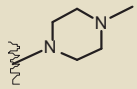	Cl	H	>100	>100
8	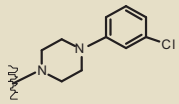	Cl	H	>100	>100
9	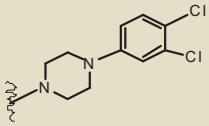	Cl	H	>100	>100
10	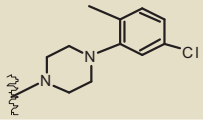	Cl	H	>100	>100
12	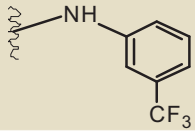	Cl	H	>30	>50
13	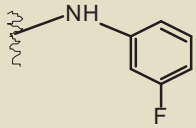	Cl	H	>30	>50
14	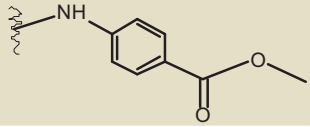	Cl	H	>30	>50

Table 2. *Continued*

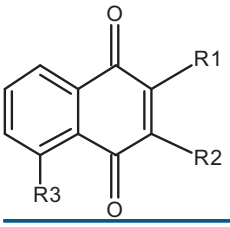

ID	R1	R2	R3	IC50 (μM) MtMetAP1a	MtMetAP1c
15	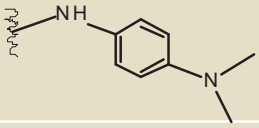	Cl	H	>30	>50
16	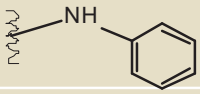	Cl	H	>50	>50
17	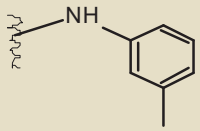	Cl	H	18.6 ± 6.1	21.3 ± 10.6
18	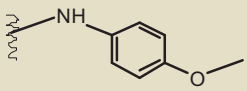	Cl	H	15.9 ± 06	22.5 ± 1.5
19	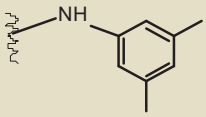	Cl	H	13.9 ± 1.0	16.4 ± 6.8
20	Br	Br	H	1.14 ± 0.25	0.71 ± 0.02
21	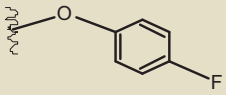	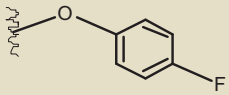	H	4.93 ± 0.20	1.79 ± 0.49
22	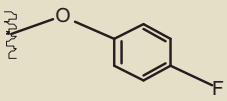	Cl	H	7.58 ± 0.28	3.74 ± 0.52
23	H	H	OH	>50	>30
24	CH_3	H	OH	>50	>50
25	OH	H	H	>50	>50
26	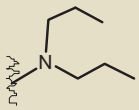	Cl	H	>50	>30
27	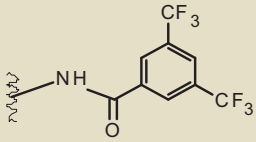	Cl	H	>50	>50
28	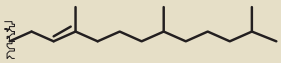	CH_3	H	>50	>50
29	CH_3	H	H	>50	>50

Table 3. Activity of *Mt*MetAP Inhibitors on *M. tuberculosis*

	Minimum Inhibitory Concentration (μg/mL)	
Compound Identification Number	Replicating *M. tuberculosis*	Aged-cultured[a] *M. tuberculosis*
2	25	23.8
3	>25	>27.6
4	10	5.7–11.4
20	10.0–25	ND
21	>25	ND
22	>25	ND

ND, not done.
[a] Nonreplicating *M. tuberculosis*.

E. coli cells (BL21) containing the expression plasmid were cultured at 37°C in 1 liter of LB containing 30 mg kanamycin until OD_{600} reached about 0.6–0.7. The expression was induced by addition of IPTG to a final concentration of 1 mM followed by shaking the culture flask at 37°C, and 275 rpm for 4 hr. The cells were harvested and washed with 1× PBS. The cells were sonicated in 1X PBS with 0.2% Triton X-100 and EDTA-free protease inhibitor tablets. The resulting cell free lysate was centrifuged at 8000× *g* for 10 min. The supernatant was loaded onto pre-equilibrated (1× PBS) Talon resin (Clontech). After equilibration for 30 min, the beads were washed three times with basic buffer (10 mM HEPES [pH 8.0], 100 mM KCl, 1.5 mM $MgCl_2$, and 10% glycerol). The enzyme was eluted with 75 mM imidazole in basic buffer. The protein was quantified using the Bradford assay. The average yield for *Mt*MetAP1c was 13.2 mg/l of culture.

Determination of Kinetic Constants of *Mt*MetAPs

The kinetic constants of the mycobacterial MetAPs were determined using a coupled methionine-proline aminopeptidase assay developed by Dr. Dehua Pei at The Ohio State University (Zhou et al., 2000). The substrate used in this assay is a dipeptide, methione-proline coupled to *p*-Nitroaniline. The dipeptide substrate, Met-Pro-*p*NA, was synthesized by Dr. Keechung Han. The kinetic constants were obtained by measuring enzyme activity at different substrate concentrations. The reactions were performed in 96-well plates at room temperature and monitored at 405 nm on a spectrophotometer. The total reaction volume was 100 μl, and each reaction contained 40 mM HEPES buffer (p.H 7.5), 100 mM NaCl, 1 μM $CoCl_2$, 100 μg/mL BSA, 0.1 U/mL ProAP, 0–800 μM substrate (Met-Pro-*p*NA), 334 nM *Mt*MetAP1c, and 3.29 μM *Mt*MetAP1a, respectively. The background hydrolysis was corrected, and the data were fitted against the Michealis-Menten equation: $V = Vmax \times [S] / (Km + [S])$, using the Graphpad prism software for one-site binding hyperbola.

High-Throughput Screening for *Mt*MetAP1c Inhibition

We screened about 175,000 compounds against MetAP1c at concentrations of 30 μM in 384-well plates, using the dipeptide substrate. The compounds were dissolved in dimethylsulfoxide (DMSO). The initial screen was conducted using a titertek instrument with liquid handling capabilities coupled to a spectrophotometer. The total reaction volume was 50 μl, and each reaction contained 40 mM HEPES buffer (pH 7.5), 100 mM NaCl, 100 μg/mL BSA, 0.1 U/mL ProAP, 1.5 mM $CoCl_2$, 600 μM substrate (Met-Pro-*p*NA), and 252 nM *Mt*MetAP1c. The enzyme was preincubated with compounds for 20 min at room temperature followed by addition of 600 μM substrate. The reaction was incubated at room temperature for 30 min and monitored at 405 nm on a spectrophotometer. The Compounds that showed greater than 30%–40% inhibition were chosen as "hits."

Determination of IC_{50} of Inhibitors of *Mt*MetAP1 and Clustering of Structural Classes of Inhibitors (ASDI-ISIS)

We determined the concentration needed for 50% inhibition in 96-well plates at final concentrations ranging from 100 μM to 300 nM (for 81 compounds that were available in larger quantities). The total reaction volume was 50 μl, and each reaction contained each *Mt*MetAP1, respectively, and 40 mM HEPES buffer (p.H 7.5), 100 mM NaCl, 100 μg/mL BSA, 0.1 U/mL ProAP, 1.5 μM $CoCl_2$, and 600 μM substrate (Met-Pro-*p*NA). The enzyme was preincubated with compounds for 20 min at room temperature followed by addition of substrate. The reaction was incubated at room temperature for 30 min and monitored at 405 nm on a spectrophotometer. The background hydrolysis was corrected, and the data were fitted against the sigmoidal-dose response (variable slope) equation using GraphPad prism software.

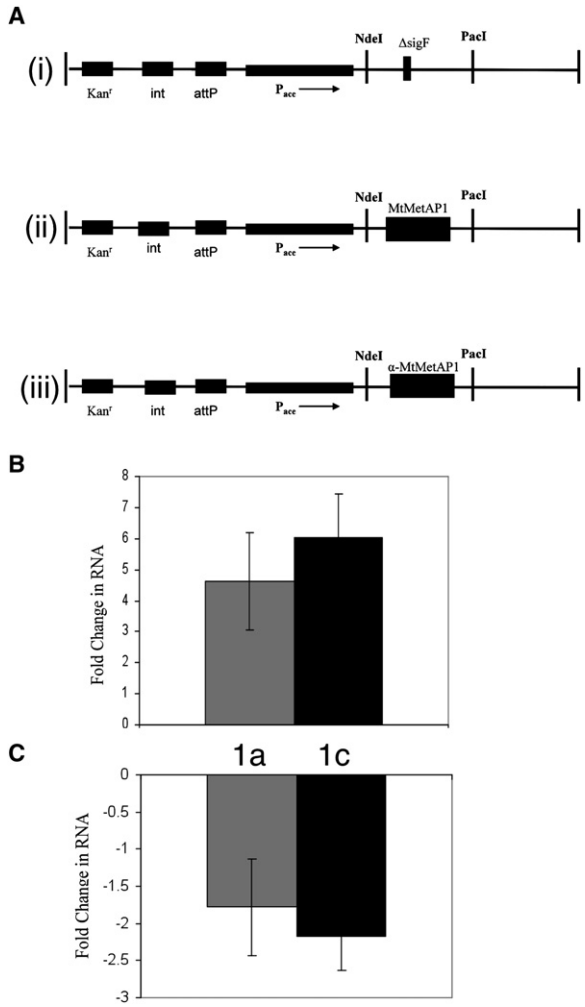

Figure 3. Overexpression of *Mt*MetAP1a and *Mt*MetAP1c Confers Resistance to Inhibitors

(A) Schematic representation of plasmids used for target validation. (i) Control plasmid pSCW35ΔsigF; (ii) sense construct: pSCW35ΔsigF-(*Mt*MetAP1); and (iii) anti-sense construct: pSCW35ΔsigF-(α-*Mt*MetAP1). The *Mt*MetAP genes were inserted downstream of the acetamide regulated promoter (P_{ace}).

(B and C) The expression of *Mt*MetAP1a and *Mt*MetAP1c mRNA in *M. tuberculosis* as determined by quantitative RT-PCR. The levels of *Mt*MetAP1a and *Mt*MetAP1c were determined in *M. tuberculosis* strains transformed with vectors overexpressing the two genes in the sense (A-ii) and antisense (A-iii) orientation, respectively. The quantities of mRNA are shown as fold change compared to the expression in the wild-type with standard error from two independent experiments.

Determination of Minimum Inhibitory Concentration in *M. tuberculosis*

The primary screen against replicating *M. tuberculosis* was conducted with 14 *Mt*MetAP inhibitors at concentrations ranging from 50 to 0.05 μg/ml. The

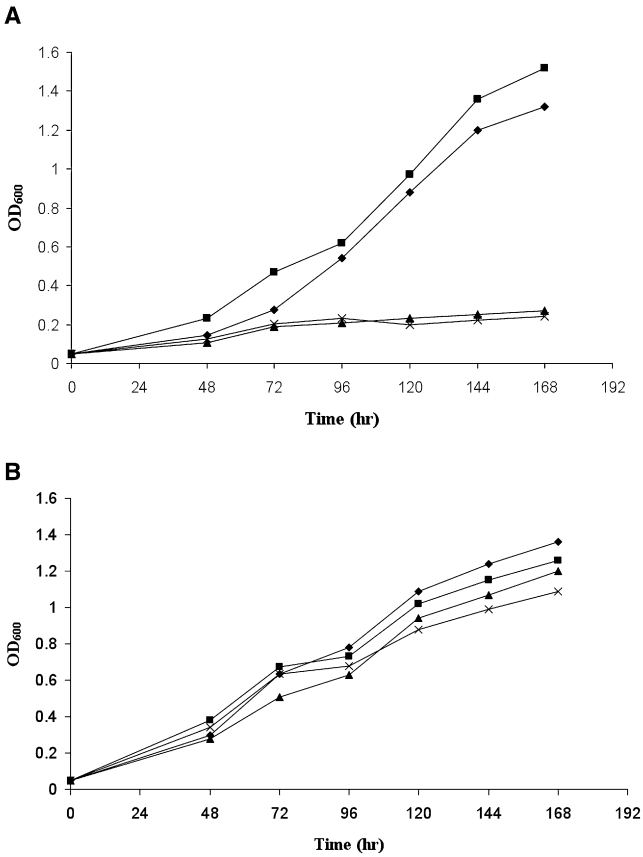

Figure 4. Target Validation of Naphthoquinone In Vivo

M. tuberculosis knock-in strains containing *Mt*MetAP1a, *Mt*MetAP1c, or control expression plasmid were grown in liquid media in the presence (A) or absence (B) of 10 μg/mL compound **4** and DMSO. Symbols: *Mt*MetAP1a, diamonds; *Mt*MetAP1c, squares; wild-type strain, stars; and sigma factor-F lacking mutant, triangles.

MetAP inhibitors were serially diluted in DMSO and added to 7H9 broth and OADC (without Tween 80) to give final concentrations of 50, to 0.05 μg/ml. A culture of *M. tuberculosis* H37Rv was grown to an OD of 1.0, and diluted to 1/100. Then each tube containing compound was inoculated with 0.1 ml of culture to give a total assay volume of 5 ml. The controls were DMSO, Isoniazid (a positive control) and a blank (drug free media). The 15-ml conical assay tubes containing mycobacteria were incubated at 37°C and in 5% CO_2. Formation of granulation was monitored for two weeks.

Activity of Inhibitors on Aged Nongrowing *M. tuberculosis*

The primary screen against non-replicating *M. tuberculosis* was conducted with 21 *Mt*MetAP inhibitors against non-replicating *M. tuberculosis* at concentrations ranging from 0.5 to 100 μM for three weeks. The screen against aged-cultured *M. tuberculosis* was conducted using a persister model, as described by Byrne et al. (2007). Briefly, a 2-month-old *M. tuberculosis* H37Ra culture grown in 7H9 medium (Difco) with 10% albumin-dextrose-catalase (ADC) and 0.05% Tween 80 was resuspended in acid 7H9 medium (pH5.5) without ADC. The bacterial cell suspension was used as inocula for assaying the activity of the compounds for persister bacilli. The compounds were diluted from the stock solution (10 mM in DMSO) to 10 μM (final) followed by incubation with the bacilli in 200 μl in acidic (pH 5.5) 7H9 medium without ADC in 96-well plates for 3 days without shaking under 1% oxygen in a hypoxic chamber. The assay was done in duplicate. Rifampin (5 μg/ml) was used as a positive control. After 3-day drug exposure, the viability of the bacilli was determined by adding 20 μl of 1 mg/ml XTT (2,3-bis-(2-methoxy-4-nitro-5-sulfophenyl)-2*H*-tetrazolium-5-carboxanilide) and incubated at 37°C up to 7 days when the plates were read at OD 485 nm.

Table 4. Viability of Knockdown Strains of *M. tuberculosis*

Knockdown Construct	Viability (%)
pSCW35-(α-MtMetAP1a)	76.0 ± 4.0
pSCW35-(α-MtMetAP1c)	95.3 ± 4.7
pSCW35ΔsigF	94.6 ± 4.4

Subcloning of *Mt*MetAP1a and *Mt*MetAP1c into pSCW35ΔsigF

The entire ORFs of *MtMetAP1a* and *MtMetAP1c* genes were amplified by polymerase chain reaction (PCR) in the sense orientation from *M. tuberculosis* strain CDC1551 genomic DNA. Then, we cloned the PCR fragments into pSCW35 vector, using the NdeI and PacI restriction sites. The primers used were as follows: for *Mt*MetAP1a, forward 5′-CGCATTAATGCCCACTGG CACGGCTGCGGGGTC-′3 and reverse 5′ CCTTAATTAACTAACCGAGCGTC AGAATTCGGGGC-′3; for *Mt*MetAP1c, forward 5′-GGAATTCCATATGCCTAG TCGTACCGCGC-′3 and reverse 5′-CCTTAATTAACTACAGACAGGTCAGG ATC-′3. The pSCW35ΔsigF-(*Mt*MetAP1a) and pSCW35ΔsigF-(*Mt*MetAP1c) clones were verified by DNA sequencing.

Overexpression of *Mt*MetAP1a and *Mt*MetAP1c in *M. tuberculosis* in the Presence of Inhibitor

We constructed knock-in strains of both *MtMetAP1*s by transforming *M. tuberculosis* CDC 1551 with pSCW35ΔsigF-(MtMetAP1a) and pSCW35ΔsigF-(MtMetAP1c), respectively. In addition, we transformed *M. tuberculosis* with a control plasmid, pSCW35ΔsigF, which is an empty vector kindly provided by Dr. Tirumalai. All three transformants were grown until early log phase and expression was induced by addition of 0.2% acetamide followed by incubation for 24 hr. We diluted the cells to an OD_{600} of 0.05 and cultured them separately in the presence of 10 μg/ml 2,3-dichloro-1,4-naphthoquinone or DMSO. Then growth was followed by recording OD_{600} every 24 hr for 7 days. The *M. tuberculosis* cultures were grown in Middlebrook 7H9 medium and supplemented with 2% glycerol, 0.05% Tween-80, and 10% albumin/dextrose complex (ADC).

Subcloning of Antisense of *Mt*MetAP1a and *Mt*MetAP1c into pSCW35ΔsigF

To study the requirement of *Mt*MetAP1a and *Mt*MetAP1c for growth and survival of *M. tuberculosis*, we cloned each of the mycobacterial MetAP1s in the reverse orientation downstream of the acetamide regulated promoter (P_{ace}) in pSCW35ΔsigF. The entire ORFs of *Mt*MetAP1a and *Mt*MetAP1c genes were amplified by polymerase chain reaction (PCR) in the antisense orientation from *M. tuberculosis* strain CDC1551 genomic DNA. Then, we cloned the PCR fragments into pSCW35ΔsigF vector, using the NdeI and PacI restriction sites. The pSCW35ΔsigF -(α-MtMetAP1a) and pSCW35ΔsigF -(α-MtMetAP1c) clones were verified by restriction digestion and DNA sequencing.

Knockdown of *Mt*MetAP1a and *Mt*MetAP1c in *M. tuberculosis*

We constructed knockdown strains of both *MtMetAP1*s by transforming *M. tuberculosis* CDC 1551 with the antisense constructs: pSCW35ΔsigF -(α-*Mt*MetAP1a) and pSCW35ΔsigF -(α-*Mt*MetAP1c). Then, we transformed *M. tuberculosis* with a control plasmid, pSCW35ΔsigF. All three transformants were grown until early log phase, and expression was induced by addition of 0.2% acetamide for 24 hr. Then the cultures were grown for three weeks on plates in the presence and absence of acetamide. The *M. tuberculosis* culture plates (Middlebrook 7H10 agar) were supplemented with 5% glycerol and 10% ADC. The colony counts were conducted after three weeks, and percentage of viability was determined using the following formula: Viability % = 100 × [number of colonies on 7H10 K15 + 0.2% acetamide / number of colonies on 7H10 K15].

Mycobacterial RNA Isolation

To confirm that the levels of both mycobacterial MetAP1s were altered as expected, we extracted RNA from the acetamide-induced transformants

and used real-time quantitative PCR to quantitate the transcript levels of both enzymes, as described below. *M. tuberculosis* cultures containing plasmids overexpressing sense and antisense constructs of *Mt*MetAP1a and *Mt*MetAP1c and the control plasmid pSCW35ΔsigF were grown to exponential phase and induced with 0.2% acetamide for 24 hr. Following induction, cells were pelleted by centrifugation at 3000 rpm for 10 min. The pellet was washed once with PBS and resuspended in 1 ml of Trizol reagent (Invitrogen Technologies) in 2 ml O-ring tubes. Cells were lysed by eight bead beating cycles of 30 s each (with 0.1 mm silica zirconia beads; Biospec Products), on a bead beater (Biospec Products). The tubes were then centrifuged at 13,000 rpm for 5 min to recover the supernatant; the beads and cell debris were discarded at this point. Two hundred microliters of chloroform was added to the supernatant and centrifuged at 13,000 rpm for 5 min following a 30 s vortex cycle. To precipitate the RNA, one volume of isopropanol was added to the aqueous phase, mixed, and incubated at RT for 10 min. RNA was pelleted by centrifuging at 13,000 rpm for 10 min at 4°C. The pellet was washed twice with 70% ethanol and dried at RT. The RNA samples were resuspended in DEPC water and quantitated by measuring A_{260}. The quality of the RNA was assessed by the A_{260} /A_{280} ratio and by agarose gel electrophoresis.

Real-Time PCR Analysis

To quantitate transcript levels of *Mt*MetAP1a and *Mt*MetAP1c under conditions where the levels of the genes was being perturbed, RNA was isolated from the acetamide-induced cultures (as described above), treated with RNase-free DNase (Ambion) and 0.5 μg of RNA, and subjected to reverse transcription using the iScript cDNA synthesis kit (Biorad). This was followed by real-time quantitative PCR using the SYBR Green Supermix (Bio-Rad Laboratories). *Mt*MetAP1a and *Mt*MetAP1c were amplified using gene specific primers; both sets of primers amplify 200 nt of the respective gene. The primers used were as follows: for *Mt*MetAP1a, forward 5′-CCGAGGTGCTC GCGCCCGGTG-3′and reverse 5′-TTCGATGGCATGCGCGACG-3′; and for *Mt*MetAP1c, forward 5′-GCTGGGCTACAAGGGATTCCCGAAG-3′ and reverse 5′ TCCGGTCAACGAGCAACCGGTG-3′. The relative fold change of mRNA of the two genes under each of the experimental conditions was measured by normalizing its transcript level to that of *M. tuberculosis* sigma factor A (*sigA*). The fold differences in transcript levels were derived by comparing the Ct values in the test (sense 1a, sense 1c, antisense 1a, and antisense 1c) samples with that of the control sample (pSCW35ΔsigF).

SUPPLEMENTAL INFORMATION

Supplemental Information includes three figures and Supplemental Experimental Procedures and can be found with this article online at doi:10.1016/j.chembiol.2009.12.014.

ACKNOWLEDGMENTS

We thank Curtis Chong, Keechung Han, Norman Morrison, Nisheeth Agarwal, and Deborah Geiman for helpful discussions. We thank ASDI Inc. for the provision of the chemical compound library. This work was supported in part by the National Institutes of Health (grants AI36973, AI37856, AI43846, and AI30036). O.O. was supported by the UNCF*Merck Graduate Science Research Dissertation Fellowship and National Aeronautics Space Administration Harriett Jenkins Pre-Doctoral Fellowship.

Received: August 4, 2009
Revised: December 9, 2009
Accepted: December 28, 2009
Published: January 28, 2010

REFERENCES

Addlagatta, A., Hu, X., Liu, J.O., and Matthews, B.W. (2005a). Structural basis for the functional differences between type I and type II human methionine aminopeptidases. Biochemistry *44*, 14741–14749.

Addlagatta, A., Quillin, M.L., Omotoso, O., Liu, J.O., and Matthews, B.W. (2005b). Identification of an SH3-binding motif in a new class of methionine aminopeptidases from *Mycobacterium tuberculosis* suggests a mode of interaction with the ribosome. Biochemistry *44*, 7166–7174.

Arfin, S.M., Kendall, R.L., Hall, L., Weaver, L.H., Stewart, A.E., Matthews, B.W., and Bradshaw, R.A. (1995). Eukaryotic methionyl aminopeptidases: two classes of cobalt-dependent enzymes. Proc. Natl. Acad. Sci. USA *92*, 7714–7718.

Bernier, S.G., Taghizadeh, N., Thompson, C.D., Westlin, W.F., and Hannig, G. (2005). Methionine aminopeptidases type I and type II are essential to control cell proliferation. J. Cell. Biochem. *95*, 1191–1203.

Boxem, M., Tsai, C.W., Zhang, Y., Saito, R.M., and Liu, J.O. (2004). The *C. elegans* methionine aminopeptidase 2 analog map-2 is required for germ cell proliferation. FEBS Lett. *576*, 245–250.

Byrne, S.T., Gu, P., Zhou, J., Denkin, S.M., Chong, C., Sullivan, D., Liu, J.O., and Zhang, Y. (2007). Pyrrolidine dithiocarbamate and diethyldithiocarbamate are active against growing and nongrowing persister *Mycobacterium tuberculosis*. Antimicrob. Agents Chemother. *51*, 4495–4497.

Chang, S.Y., McGary, E.C., and Chang, S. (1989). Methionine aminopeptidase gene of *Escherichia coli* is essential for cell growth. J. Bacteriol. *171*, 4071–4072.

Chang, Y.H., Teichert, U., and Smith, J.A. (1992). Molecular cloning, sequencing, deletion, and overexpression of a methionine aminopeptidase gene from *Saccharomyces cerevisiae*. J. Biol. Chem. *267*, 8007–8011.

Chen, X., Chong, C.R., Shi, L., Yoshimoto, T., Sullivan, D.J., Jr., and Liu, J.O. (2006). Inhibitors of *Plasmodium falciparum* methionine aminopeptidase 1b possess antimalarial activity. Proc. Natl. Acad. Sci. USA *103*, 14548–14553.

Cole, S.T., Brosch, R., Parkhill, J., Garnier, T., Churcher, C., Harris, D., Gordon, S.V., Eiglmeier, K., Gas, S., Barry, C.E., 3rd., et al. (1998). Deciphering the biology of *Mycobacterium tuberculosis* from the complete genome sequence. Nature *393*, 537–544.

Dye, C. (2006). Global epidemiology of tuberculosis. Lancet *367*, 938–940.

Fauci, A.S. (2008). Multidrug-resistant and extensively drug-resistant tuberculosis: the National Institute of Allergy and Infectious Diseases Research agenda and recommendations for priority research. J. Infect. Dis. *197*, 1493–1498.

Gandhi, N.R., Moll, A., Sturm, A.W., Pawinski, R., Govender, T., Lalloo, U., Zeller, K., Andrews, J., and Friedland, G. (2006). Extensively drug-resistant tuberculosis as a cause of death in patients co-infected with tuberculosis and HIV in a rural area of South Africa. Lancet *368*, 1575–1580.

Giglione, C., Vallon, O., and Meinnel, T. (2003). Control of protein life-span by N-terminal methionine excision. EMBO J. *22*, 13–23.

Griffith, E.C., Su, Z., Turk, B.E., Chen, S., Chang, Y.-W., Wu, Z., Biemann, K., and Liu, J.O. (1997). Methionine aminopeptidase (type 2) is the common target for angiogenesis inhibitors AGM-1470 and ovalicin. Chem. Biol. *4*, 461–471.

Hu, X., Addlagatta, A., Lu, J., Matthews, B.W., and Liu, J.O. (2006). Elucidation of the function of type 1 human methionine aminopeptidase during cell cycle progression. Proc. Natl. Acad. Sci. USA *103*, 18148–18153.

Li, X., and Chang, Y.H. (1995). Amino-terminal protein processing in *Saccharomyces cerevisiae* is an essential function that requires two distinct methionine aminopeptidases. Proc. Natl. Acad. Sci. USA *92*, 12357–12361.

Lowther, W.T., and Matthews, B.W. (2000). Structure and function of the methionine aminopeptidases. Biochim. Biophys. Acta *1477*, 157–167.

Miller, C.G., Kukral, A.M., Miller, J.L., and Movva, N.R. (1989). pepM is an essential gene in *Salmonella typhimurium*. J. Bacteriol. *171*, 5215–5217.

Narayanan, S.S., Ramanujan, A., Krishna, S., and Nampoothiri, K.M. (2008). Purification and biochemical characterization of methionine aminopeptidase (MetAP) from *Mycobacterium smegmatis* mc2155. Appl. Biochem. Biotechnol. *151*, 512–521.

Raghunand, T.R., Bishai, W.R., and Chen, P. (2006). Towards establishing a method to screen for inhibitors of essential genes in mycobacteria: evaluation of the acetamidase promoter. Int. J. Antimicrob. Agents *28*, 36–41.

Raviglione, M.C. (2003). The TB epidemic from 1992 to 2002. Tuberculosis (Edinb.) *83*, 4–14.

Ribeiro-Guimaraes, M.L., and Pessolani, M.C. (2007). Comparative genomics of mycobacterial proteases. Microb. Pathog. *43*, 173–178.

Sin, N., Meng, L., Wang, M.Q., Wen, J.J., Bornmann, W.G., and Crews, C.M. (1997). The anti-angiogenic agent fumagillin covalently binds and inhibits the methionine aminopeptidase, MetAP-2. Proc. Natl. Acad. Sci. USA *94*, 6099–6103.

Solbiati, J., Chapman-Smith, A., Miller, J.L., Miller, C.G., and Cronan, J.E., Jr. (1999). Processing of the N termini of nascent polypeptide chains requires deformylation prior to methionine removal. J. Mol. Biol. *290*, 607–614.

Yeh, J.R., Ju, R., Brdlik, C.M., Zhang, W., Zhang, Y., Matyskiela, M.E., Shotwell, J.D., and Crews, C.M. (2006). Targeted gene disruption of methionine aminopeptidase 2 results in an embryonic gastrulation defect and endothelial cell growth arrest. Proc. Natl. Acad. Sci. USA *103*, 10379–10384.

Zhang, Y. (2005). The magic bullets and tuberculosis drug targets. Annu. Rev. Pharmacol. Toxicol. *45*, 529–564.

Zhang, X., Chen, S., Hu, Z., Zhang, L., and Wang, H. (2009). Expression and characterization of two functional methionine aminopeptidases from *Mycobacterium tuberculosis* H37Rv. Curr. Microbiol. *59*, 520–525.

Zhou, Y., Guo, X.C., Yi, T., Yoshimoto, T., and Pei, D. (2000). Two continuous spectrophotometric assays for methionine aminopeptidase. Anal. Biochem. *280*, 159–165.

Zignol, M., Hosseini, M.S., Wright, A., Weezenbeek, C.L., Nunn, P., Watt, C.J., Williams, B.G., and Dye, C. (2006). Global incidence of multidrug-resistant tuberculosis. J. Infect. Dis. *194*, 479–485.